

Physical Processes in Azobenzene Polymers on Irradiation with Polarized Light

N. C. R. Holme, L. Nikolova, T. B. Norris, S. Hvilsted, M. Pedersen, R. H. Berg, P. H. Rasmussen and P. S. Ramanujam*

Risø National Laboratory, DK-4000 Roskilde, Denmark

SUMMARY: Azobenzenes can serve as model compounds for the study of *trans-cis* isomerization in more complex molecules. We have performed time-resolved spectroscopy in solutions containing free azobenzene chromophores and diols with a view to obtaining the energy levels and lifetimes of the excited states. A transition route based on experimental results for the theoretically calculated energy level scheme is proposed. Physical observations of surface relief in thin films of azobenzene polymers when irradiated with polarized light are reported. These include two beam polarization holographic observations and single beam transmission measurements through a mask, followed by atomic force microscope and profiler investigations. It is concluded that none of the prevalent theories can explain all the observed facts.

Introduction

Trans-cis isomerization processes play an important role in nature, such as in the field of vision¹⁾. Azobenzenes with their simple structure serve as model compounds for investigating these isomerization processes. During such an isomerization, the molecule physically alters its dimensions, giving rise to interesting physics²⁾. Generally, the *trans-cis* isomerization has been found to be rapid, on the order of a few ps. The *cis* state can isomerize back to the *trans* state either through a thermal process or a light induced process. An important parameter for the determination of the spectral and temporal response of such systems is an understanding of the energy levels of azobenzene. To date there is little known experimentally about the energy levels of azobenzene, especially the ordering of the triplet levels.

Recently, polymers in which azobenzenes are attached in the main or side chains, have been found to have great potential for optical information storage³⁻¹⁰⁾. Optical storage based on azobenzene has been achieved both in guest-host systems and in systems with the azobenzene

bonded to the polymer structure. One of the most intriguing discoveries in polymers with azobenzene in side or main chains is the appearance of a surface relief on irradiation with laser beams. Initial experiments have been performed with two coherent argon ion laser beams in a holographic set-up with the same polarization^{11, 12)}. We have shown that a strong surface relief arises even in a polarization holographic set-up with orthogonally polarized beams¹³⁾ when no intensity modulation takes place. In fact, experiments performed even with single laser beams incident at an angle to the film, breaking the s-p symmetry show a pronounced surface relief¹⁴⁾.

Two different studies on the azobenzene polymers are reported in this article. The first study reports time-resolved spectroscopy of azobenzene in a solution. The aim of this research is to determine the lifetimes of the excited states in the *trans* state of the azobenzene, as well as to determine a path to isomerization. In the second part of the article, we discuss the nature of the surface relief obtained, when an azobenzene containing film is irradiated with one or more polarized light beams. We show that the nature of the surface relief is different in the different polymers studied, depending on their architecture.

Several side-chain polymers have been examined in the current study - side-chain liquid crystalline polyesters, polyesters with a chiral substituent on the azobenzene, polyesters with a rigid main chain, methacrylate co-polymer systems with 20 to 100% azobenzene concentration, azobenzene peptide oligomers and a methacrylate polymer with disperse red.

Synthesis

The synthesis of the azobenzene chromophore with different substituents has been discussed by Pedersen¹⁵⁾. The structure of the cyanoazobenzene in a diol configuration and as a free chromophore is shown in Fig. 1. The synthesis of the side-chain liquid crystalline polyesters has been discussed in Ref.16, methacrylate co-polymer systems in Ref. 17, peptide oligomers in Ref. 18 and methacrylate polymer with disperse red in Ref. 19.

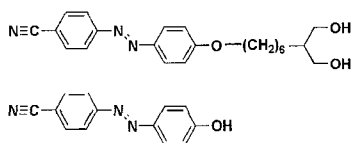


Fig. 1: The structure of the cyanoazobenzene in a diol and as a chromophore.

Instrumentation

Thin films of the polymers have been obtained by dissolving the polymers in suitable solvents (chloroform, THF or trifluoroacetic acid-hexafluoroisopropanol) through either solution casting or spin-coating on glass substrates. Thicknesses of the films varied between 2 and 10 μm as measured with a Dektak 3030 profile measuring system.

Time-resolved spectroscopy

The mechanism of the isomerization of azo compounds has not been unambiguously determined. Both a rotation and an inversion path have been proposed²⁰⁻²³. An energy level diagram for CN substituted azobenzene based on recent calculations²⁴ using a Pariser-Parr-Pople (PPP) model supplemented with perturbation analysis is shown in Fig. 2.

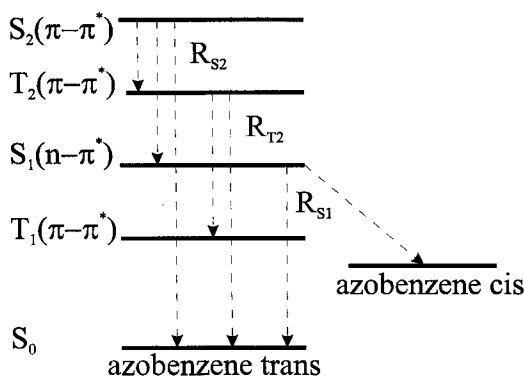


Fig. 2: The transition routes considered in the rate equation model.

Measurements of quantum efficiency for the *trans-cis* isomerization have shown that the isomerization yield upon excitation to the $S_2(\pi-\pi^*)$ is only half of what is obtained upon excitation to the $S_1(n-\pi^*)$ ^{22,25}. It is thus reasonable to assume that there exists a path from the S_2 state to the *trans* ground state, not involving the $S_1(n-\pi^*)$ – but possibly involving the T_1 and T_2 triplet states.

Relatively few measurements have been made on the time-resolved spectroscopy of azobenzene. The time resolved emission from the $S_1(n-\pi^*)$ excited states of azobenzene has

been studied by Struve²⁶⁾, using a wavelength of 531 nm for excitation of *trans*-azobenzene dissolved in cyclohexane. It was found that the fluorescence signal had a decay time of ~ 25 ps. Morgante and Struve²⁷⁾ also studied time resolved emission from the $S_2(\pi-\pi^*)$ state of the excited azobenzene, using 354 nm for excitation, and found that the fluorescence from the S_2 state has a lifetime of less than 5 ps²⁷⁾. Hamm et al. used time resolved IR spectroscopy to study the vibrational cooling of photoisomerized azobenzene molecules²⁸⁾. Here a wavelength of 408 nm was used for the excitation of the $S_2(\pi-\pi^*)$ state. The vibrational spectra were probed between 1400 and 1550 cm^{-1} . Lednev et al.²⁵⁾ have performed time resolved absorption spectroscopy on azobenzene dissolved in hexane, cyclohexane, hexadecane and acetonitrile, using a 303 nm pump. This again pumps the $S_2(\pi-\pi^*)$ state. The probe wavelengths in this case were between 303 nm and 500 nm. The observed time resolved changes in the absorption could in all cases be fitted with a double exponential decay, with decay times on the order of 1 ps and 13 ps. From these data, the presence of a bottleneck state was suggested. Within the accuracy of the measurements, no correlation between solvent viscosity and lifetimes was observed, and only a weak dependency was found between the solvent dielectric constant and the lifetimes.

Experimental set-up for degenerate measurement

Two types of experiments will be described in this section. In the first experiment we performed degenerate pump-probe measurements at a wavelength of 400 nm. The setup for this part is shown in Fig.3.

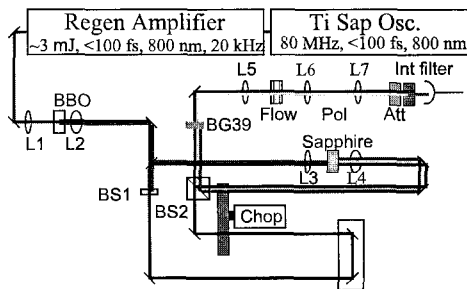


Fig. 3: Experimental set-up to perform the degenerate pump-probe measurements

Pulses from a Ti-Sapphire oscillator²⁹⁾ are amplified in a regenerative amplifier³⁰⁾, to produce 800 nm pulses, (pulse width less than 100 fs), with a pulse energy of about 3 μJ , at a repetition rate of 20 kHz. The light is frequency doubled using a BBO crystal, and residual

800 nm light is rejected using a color filter. A small fraction of the blue light (the probe beam) is reflected of a beam splitter (BS1), and directed toward a fixed delay arm, the main part of the 400 nm light (the pump beam) going to a variable delay. The pump and the probe beam are chopped at 700 and 1600 Hz, before the two beams are directed collinearly towards the sample cell. The polarization of the probe beam can be controlled using wave plates. In this way we can measure the signal with the polarization state of the pump and the probe beam either parallel or perpendicular to each other. The two beams are tightly focused onto the flow cell (a 1 mm path length quartz flow cell) using a 50 mm lens, then collimated again, before the pump beam is blocked with an aperture. After a neutral density filter, the probe beam is focused onto a detector. The output from the detector is fed to a lock-in amplifier, which is referenced to the sum of the two chopping frequencies (2.3 kHz). The double chopping scheme is used in order to avoid problems with detecting scattered pump light. The flow system used for these measurements was composed of a gear-driven pump, a glass bottle for reservoir, and teflon tubing and fittings.

Non-degenerate measurement

This set-up was the same as the previous set-up, apart from the fact that in this set-up the residual 800 nm light from the frequency doubling was used to generate white light in a sapphire crystal in the probe beam arm. A polarizing beam splitter was used to overlap the pump and the probe beam, and finally a series of interference filters were used to select different probe wavelengths.

Data treatment

Due to the low pulse energy we had to focus both the pump- and the probe beam tightly in the sample volume, in order to obtain a suitable signal to noise ratio. Unfortunately the

consequence of this is that we cannot determine the absolute values of $\frac{\Delta A}{I_{pump}}$, where I_{pump} is the pump intensity, and ΔA is the induced change in absorbance. All the data presented are therefore normalized.

Recent measurements of the $N=N$ stretching mode on unsubstituted azobenzene have shown that the depolarization ratios are very close to 1/3 for wavelengths in the range from 445 to 570 nm³¹⁾. We have thus used the following equation to calculate the anisotropy of the sample

$$a = \frac{3\Delta A_{\parallel} - \Delta A_{\perp}}{3\Delta A_{\parallel} + 2\Delta A_{\perp}} \quad (1)$$

where ΔA_{\parallel} and ΔA_{\perp} are the normalized change in absorbance for probe polarized parallel and perpendicular to the pump beam. In order to determine the sign of ΔA , measurements were performed with only the pump beam chopped. A small fraction of the pump beam was allowed to strike the detector, (thus allowing us to set the phase of the lock-in amplifier), by monitoring the change in the lock-in signal as the probe beam was blocked/unblocked, the sign of ΔA could be determined.

Results and Discussion

Experiments have been performed on a series of substituted azobenzene chromophores using NO_2 , CN and Phenyl as substituents. The degenerate measurements were performed with the polarization of the probe beam parallel and perpendicular to the pump polarization, as this

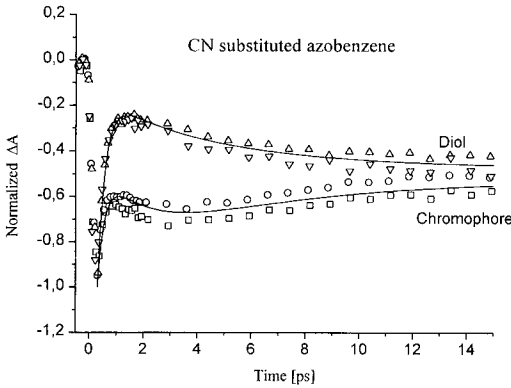


Fig. 4: Experimental data (points) and theoretical fits (solid curves) to the change in normalized absorption for the case of cyanoazobenzene chromophores and in a diol.

allows us to examine not only the change in absorption, but also examine the decay of the induced anisotropy in the sample. The non-degenerate measurements were only performed using perpendicular polarization, as the degenerate measurements only showed minor contributions from the anisotropy term, during the first 10 ps, after the pump pulse.

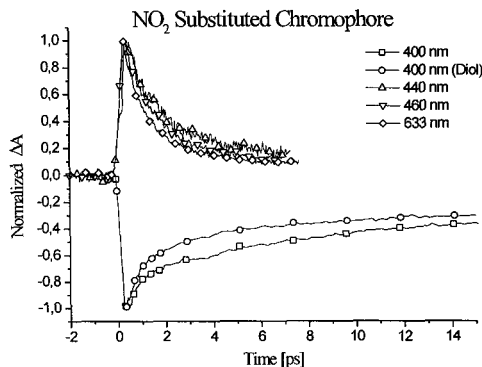


Fig. 5: Experimental data (points) and theoretical fits (solid curves) to the change in normalized absorption for the case of nitro-substituted chromophores and in a diol.

In Fig. 4, the normalized ΔA signal is shown for the CN substituted azobenzene. In Fig. 5 the normalized ΔA signal is shown for the NO_2 substituted azobenzene, for different probe wavelengths, and for the 400 nm probe wavelength with the polarization of the probe beam

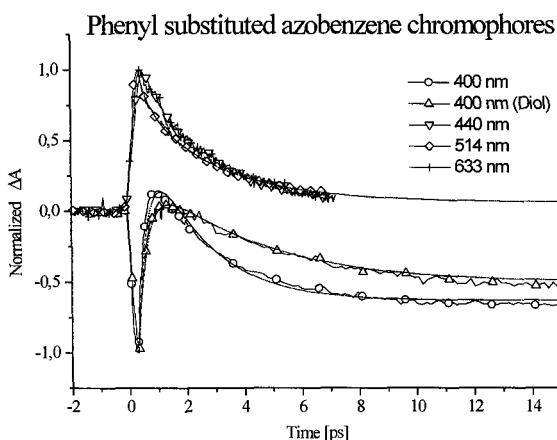


Fig. 6: Experimental data (points) and theoretical fits (solid curves) to the change in normalized absorption for the case of phenyl substituted chromophores and in a diol.

perpendicular to the pump beam. There is a tendency to a faster decay for longer probe wavelengths, which has also been observed by Lednev et al.²⁵⁾ in unsubstituted azobenzene.

We find that the attachment of the chromophore to the polymer does not change the characteristics of the chromophore substantially. This is an important observation, as this means that we can expect the results obtained from the substituted chromophore will also apply to the final polymer structure. In Fig. 6, the normalized ΔA is shown for the phenyl substituted azobenzene. In this case all the probe wavelengths apart from the 400 nm shows almost the same behavior. We have also observed in this case that there is no substantial difference between the chromophore alone and as attached to a side-chain.

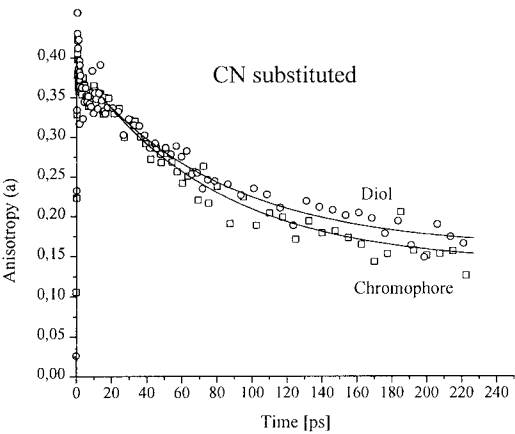


Fig. 7: Anisotropy in CN substituted azobenzene chromophore and diol.

Theoretical analysis

Using eqn. (1), we have calculated the anisotropy for the different samples in the degenerate case. An example of this for CN substituted chromophore and diol is shown in Fig. 7. For $t > 20$ ps, these curves can be fitted fairly well with a single exponential. The decay time constants τ , for the anisotropy found from a single exponential fits are shown in Table 1.

Tab.1. Decay constants for substituted free chromophores and those attached to a side-chain

Substituent	τ [ps] (substituted chromophore)	τ [ps] (attached to side-chain)
CN	77	80
NO ₂	71	97
Phenyl	89	117

It is seen that there is tendency of increased time constants for larger substituents. There is also an increase in the time constants for the case of chromophores attached to a side-chain, which might be due to the fact that molecular mobility is reduced for larger systems.

Kinetics

We have set up a model to describe the observed data. From the literature we know that

- 1) Measurements of quantum yields for *trans-cis* isomerization ϕ_{t-c} upon $S_1(n-\pi^*)$ and $S_2(\pi-\pi^*)$ excitation has been reported, and it is found that the quantum yield upon $S_1(n-\pi^*)$ excitation is about twice the value obtained upon $S_2(\pi-\pi^*)$ ²²⁾.
- 2) Earlier time resolved fluorescence of the $S_1(n-\pi^*)$ excited *trans* azobenzene showed lifetimes of the order of 25 ps²⁶⁾.
- 3) Recently, Lednev. et al. reported time-resolved absorption measurements on $S_2(\pi-\pi^*)$ excited unsubstituted *trans* azobenzene, in this study lifetimes of 1 ps and ~13 ps was observed²⁵⁾.
- 4) Measurements of quantum yield for *trans-cis* isomerization upon excitation into both the $S_1(n-\pi^*)$ and the $S_2(\pi-\pi^*)$ band, performed by Bourtolus and Monti³²⁾, indicate that isomerization takes place either directly from the S_1 or a state reached from the S_1 state.
- 5) Measurements using triplet energy donors, with $E_T \geq 45.3$ kcal/mol showed that these donors could not sensitize the *trans-cis* isomerization, whereas *cis-trans* isomerization could be sensitized with unity quantum yield. From these studies it was concluded that photo isomerization occurs in the singlet manifold³²⁾.

In order to explain the observed behavior we suggest the following scheme. After excitation to the S_2 state a rapid depopulation of the S_2 state, through decays to the S_0 , S_1 , and T_2 states, takes place. All the molecules excited to the S_2 state cannot decay through the S_1 state since the quantum yield for *trans-cis* isomerization upon $S_2(\pi-\pi^*)$ excitation is only half of what is obtained upon $S_1(n-\pi^*)$ excitation. The population of the T_2 state is supported by the following argument:

From Fig.6, it can be seen that after the depopulation of the S_2 state another rapid transition is taking place. This cannot be a depopulation of the S_1 state, through an S_1-T_1 transition, as the T_1 state is known not to isomerize³²⁾. On the other hand a T_2-T_1 transition would be expected

to be fast, as observed, whereas both S_1 - T_1 and T_1 - S_0 transitions would be expected to be very slow (on this timescale). Thus we believe that the final product we observe consists of ground state *trans* and *cis* azobenzene, and T_1 excited azobenzene, with a long lifetime.

We have modeled the data by setting up a set of rate equations describing a six level system. The states involved are the ground state of the *trans* configuration t - S_0 , the directly excited *trans* configuration t - S_2 , two intermediate *trans* states, t - S_1 and t - T_2 , and finally the *cis* ground state and the *trans* T_1 state. According to the assumptions the t - S_2 state will decay to the t - T_2 , t - S_1 , and t - S_0 states, with a rate R_{S_2} . The t - T_2 state decays to the t - T_1 and the t - S_0 state with a rate R_{T_2} . The t - S_1 state decays to the t - S_0 and the *cis* state, with a rate R_{S_1} . The branching between the different states is denoted by σ , where σ_{a-b} denotes the probability that a molecule decaying from state a will decay to state b . The rate equations to be solved are shown below, where n_x denotes the population of molecules in the x state, with the initial condition $n_{S_2}(0)=1$.

$$\frac{dn_{S_2}}{dt} = -R_{S_2} n_{S_2}$$

$$\frac{dn_{S_1}}{dt} = \sigma_{S_2-S_1} R_{S_2} n_{S_2} - R_{S_1} n_{S_1}$$

$$\frac{dn_{T_2}}{dt} = \sigma_{S_2-T_2} R_{S_2} n_{S_2} - R_{T_2} n_{T_2}$$

$$\frac{dn_{cis_1}}{dt} = \sigma_{S_2-cis} R_{S_2} n_{S_2}$$

$$\frac{dn_{T_1}}{dt} = \sigma_{T_2-T_1} R_{T_2} n_{T_2}$$

$$\frac{dn_{S_0}}{dt} = \sigma_{S_2-S_0} R_{S_2} n_{S_2} + \sigma_{S_1-S_0} R_{S_1} n_{S_1} + \sigma_{T_2-S_0} R_{T_2} n_{T_2}$$

The absorbance of the sample is given by the following equation:

$$A = A_{S_0} n_{S_0} + A_{S_1} n_{S_1} + A_{S_2} n_{S_2} + A_{T_1} n_{T_1} + A_{T_2} n_{T_2} + A_{cis} n_{cis}$$

As the absorbance of the excited states is not known at present we can not determine the branching ratios and thereby the quantum efficiency for the photo-isomerization, but the rates can be determined from the fitting procedure. These results are shown in Table 2. The

measured data and the fitted curves for different probe wavelengths are shown in Figs. 4, 5 and 6. In this case, the rates are kept fixed and only the absorbance of the different states has been varied for the different probe wavelengths.

Tab.2. Rate constants

Sample	$1/R_{s2}$ [ps]	$1/R_{T2}$ [ps]	$1/R_{s1}$ [ps]
NO ₂ 400/630 nm probe	1.0	2.0	10.0
NO ₂ -diol 400 nm probe	1.0	2.0	10.0
Phenyl 400/514 nm probe	0.5	3.3	20.0
Phenyl- diol 400 nm probe	0.5	2.0	10.0
CN 400 nm probe	0.33	2.0	10.0
CN-diol 400 nm probe	0.5	5.0	20.0

Surface relief in thin azobenzene polymer films

For the study of anisotropy and surface relief in the films, a polarization holographic system was used. Two beams from an argon ion laser at 488 nm were allowed to overlap in the film, and the inscribed grating was probed with a HeNe laser at 633 nm. The plane of incidence is horizontal in all the experiments described below. The polarization of the write beams could be changed to vertical-horizontal, $\pm 45^\circ$ and orthogonal circular configurations. Similarly the polarization of the read beam could be chosen to be linear or circular. In almost all cases, we found that a topographic relief appears in addition to the anisotropic grating. The topographic grating appears to be extremely stable. In the case of peptide oligomers, the grating is not erased even at 210 °C. Long term measurements of anisotropy in amorphous azobenzene polymers induced with a single beam, show a complete decay of the anisotropy in approximately 20000 minutes³³). However surface relief gratings written in these films are stable over a period of years.

We have been able to separate the anisotropic (polarization) properties of the gratings from that of the isotropic (surface-relief) properties. In this case, the gratings were written with orthogonal circular polarization and the read beam was polarized vertically or horizontally. The first order diffracted beam was split into horizontally and vertically polarized components through a Wollaston prism and the two beams were detected individually as a function of

time. Through the use of Jones' calculus, the contributions to the diffraction efficiency from anisotropy and surface relief can be calculated³⁴⁾.

The gratings obtained above have also been examined with a TopoMetrix Explorer atomic force microscope. Atomic force microscopic measurements have also been performed in these films after they have been irradiated through a transmission-grating mask. The period of the grating was 30 μm while the width of the transmitting areas varied between 2 μm and 25 μm . The irradiation in this case was performed with an argon ion laser at 488 nm with vertical, horizontal or circular polarization.

All polymers containing azobenzene in side and/or main chains have been found to exhibit a strong regular relief when irradiated with two polarized beams of light. Even a single beam of light incident at an angle to the film surface so as to break the s-p symmetry has been found to give a large roughness of the surface depending on the polarization of the incident light¹⁴⁾.

Calculation of the diffraction efficiency with anisotropy and surface relief

We have shown³⁴⁾ that the contributions of anisotropy and surface relief to the diffraction efficiency can be estimated through a measurement of the first order diffraction efficiency as follows. The grating is written with two orthogonally circularly polarized beams and is probed using a linearly polarized HeNe laser beam. The first order diffracted beam is split into a horizontal (H) and a vertical (V) component using a Wollaston prism. Using Jones calculus, the intensities of the two beams after the Wollaston prism are

$$I_{vv} = \left| a + be^{i\delta_0} \right|^2 = a^2 + b^2 + 2ab \cos \delta_0$$

$$I_{vh} = a^2$$

Here the first index v refers to the vertical polarization of the probe beam and the second indices v, h refer to the vertical and horizontal component of the diffracted wave.

For horizontal polarization of the probe beam we obtain:

$$I_{hh} = \left| -a + be^{i\delta_0} \right|^2 = a^2 + b^2 - 2ab \cos \delta_0$$

$$I_{hv} = a^2$$

Thus, by measuring the intensities I_{vv} , I_{vh} , I_{hh} and I_{hv} we can find a , b and δ_0 . In the above equations, $a = \sin(\Delta\phi)/2$, and $b = \cos(\Delta\phi)J_1(\Delta\psi)$. Here, $\Delta\phi = \pi(\delta n)d/\lambda$ is the anisotropic phase shift due to the induced birefringence δn , d is the film thickness and λ is the wavelength. $\Delta\psi = \pi(\Delta n)(\Delta d)/\lambda$, Δn is the difference between the refractive index of the polyester and air and $(2\Delta d)$ is the relief height. $J_1(\Delta\psi)$ is the first order Bessel function of the first kind in $\Delta\psi$. δ_0 is the displacement between the anisotropic and topographic gratings; $\delta_0=0$ corresponds to the valley of the surface grating corresponding to the horizontal direction in the polarization pattern. The values of $\Delta\phi$ and $\Delta\psi$ can thus be determined.

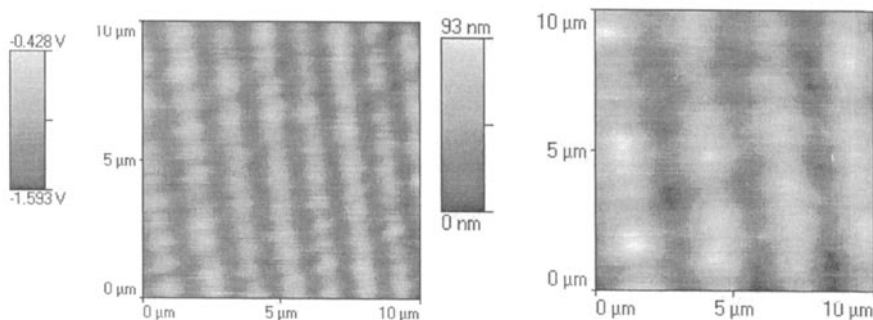


Fig. 8: Anisotropic and topographic grating in the side-chain liquid crystalline polyester, **P6a12**.

It is found that in the case of side-chain liquid crystalline polyesters, the valley of the topographic grating coincides with the vertical polarization of the recording field, while in the case of all amorphous polymers we have investigated, the valley of the topographic grating coincides with the horizontal polarization at moderate fluence. However, most intriguing surface relief patterns have been found when a film of **pDR1A** is irradiated with two orthogonally circularly polarized beams for different lengths of time. (**pDR1A** is a disperse-red containing polyacrylate system – the material was kindly given by Dr. Paul Rochon). It is seen that an initial smooth growth of a surface relief grating develops into a rough growth between the peaks for intermediate irradiation times and finally into more ordered, herringbone like, spherule structures. Material is not just transported, but rather aggregates into regular structures.

These results show that the formation of the surface relief is related to the photoinduced ordering in the polymer film and is dependent on the modulation of the direction of the photoinduced axes of symmetry.

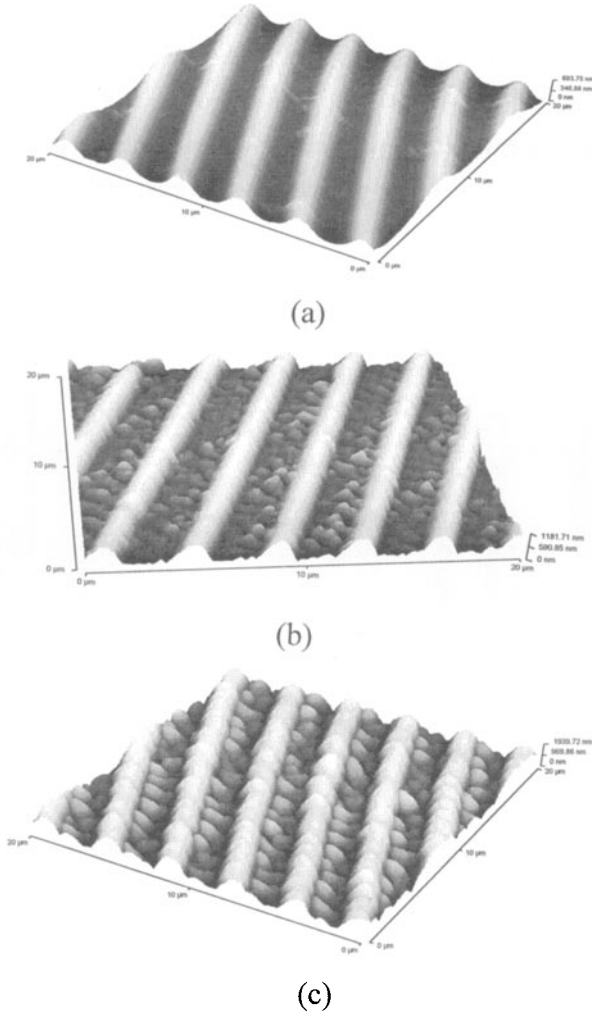


Fig. 9: AFM scans of **pDRIa** after exposure to two orthogonally circularly polarized argon laser beams at an intensity of 3 W/cm^2 for 60 s, 180 s and 300 s respectively. The scanned area is $20 \mu\text{m} \times 20 \mu\text{m}$. Maximum surface relief in (a) is 600 nm, in (b) is 1200 nm and in (c) is 2000 nm.

When the polarizations of the recording beams are vertical and horizontal, the symmetry of the photoinduced ordering is quite different, the induced axes are at $+45^\circ$ and -45° . AFM scans of these gratings reveal the appearance of a surface relief with double frequency³⁵⁾. The double-frequency surface relief is found to be shifted by $\pi/4$ with respect to the interference pattern. This phase shift is explained as due to the influence of the $+1$ and -1 order diffracted waves during the real time recording. These diffracted waves change the initial polarization

modulation in such a way that the induced axes are along the grating vector twice in a grating period for phase shifts of $\pi/4$ and $5\pi/4$. AFM measurements of other azobenzene polymers after holographic recording with horizontal/vertical polarized light reveals a variety of relief shapes with both normal and doubled frequency depending on the type of the polymer, the recording intensity and the exposure time. Thus one has to be very careful in the application of the Jones calculus for the analysis of surface relief and anisotropy. A complete analysis of the grating structure should be based on linear and circular anisotropy in the films, the presence of higher order surface relief and the influence of the first order diffracted waves³⁵.

Experimentally it has been found that the appearance of the surface relief is very rapid. Surface relief profiles have been fabricated in an aromatic azobenzene polyester with just one 5 ns pulse from a frequency doubled YAG laser in a polarization holographic set-up.

Irradiation experiments with a transmission mask

In order to investigate the reason for the different displacement between the anisotropic and topographic grating, we have performed irradiation experiments through a transmission mask. The mask consists of a periodic amplitude grating, with a period of 30 μm with the width of the transparent region being 5 μm . The liquid crystal polyester film **P6a12** was placed on the grating, and was irradiated with polarized light. With linearly polarized light with the electric field vector perpendicular to the grating vector (i. e., polarized parallel to the grating lines), atomic force microscopic investigations revealed the presence of topographic features consisting of weak maxima. On irradiation with the orthogonally linearly polarized light (i.e., polarized perpendicular to grating lines), strong and broad maxima were obtained. Circularly polarized light produced sharp and strong maxima. The experiments were repeated for the case of **P6a4**, which is in the smectic phase at room temperature. The results show again that peaks are formed in areas illuminated with light polarized parallel to the grating vector.

However, similar experiments performed on amorphous side-chain polyesters, methacrylate systems and peptide oligomers, showed very deep trenches on extended irradiation with light polarized perpendicular to the grating lines. Irradiation performed with circularly polarized light produced also trenches, while light polarized parallel to the grating lines once again produced weak maxima. Fig. 10 shows AFM scans of the liquid crystalline polyester **P6a12** after irradiation through the mask with polarization parallel to the grating vector. The same situation is shown in the case of a peptide oligomer that is amorphous in Fig. 11.

We found that in the latter case, the nature of the surface relief depends on the intensity of the irradiating light. For small intensities ($\sim 100 \text{ mW/cm}^2$), broad peaks are obtained and for high intensities (1 W/cm^2), trenches are created. Intermediate values of the intensities produce both troughs and peaks. Subtle structural changes in the polymer architecture, such as

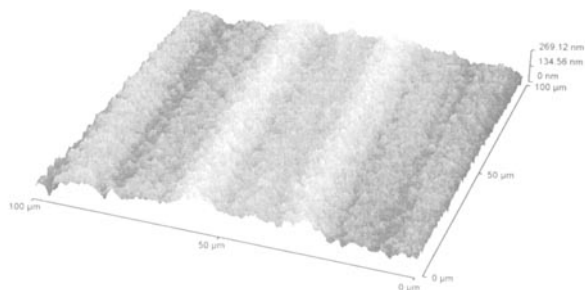


Fig. 10: Mask irradiation - **P6a12** - Linear polarization parallel to grating vector

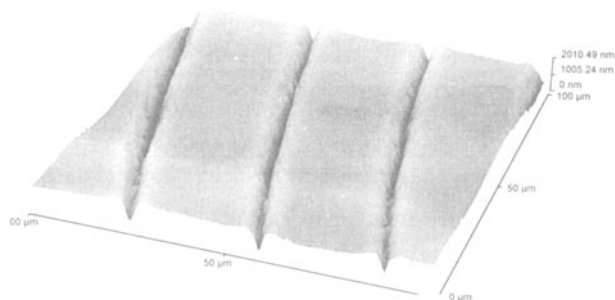


Fig. 11: Mask irradiation - **DNO-137** - Linear polarization parallel to grating vector

changing from an aliphatic main chain to an aromatic main chain produce dramatic changes. Thus in the case of **P6aA** which is an amorphous aromatic polyester, for light polarized parallel to the grating vector, when the scan is performed at the edge of the gaussian profile, peaks are obtained (Fig. 12). Moving towards the centre, we have a splitting of the peaks, and finally holes are obtained (Fig. 13, Fig. 14). Since the surface relief depends on the incident fluence, this observation implies that the peaks evolve into trenches as a function of time. Extending this conclusion to the case of polarization holography, this leads to a time dependent displacement (phase shift) between the anisotropic and topographic grating, which may explain the decrease in diffraction efficiency observed by Jiang et al.³⁶⁾. It should be noted that this phenomenon does not occur in the case of the liquid crystalline polyesters.

Fig. 15 shows AFM scans performed on **P6a12** and the amorphous polyester **P6aA** with azobenzene side-chains after irradiation with horizontal polarization (polarization parallel to the grating vector) showing that both peaks and trenches can be obtained.

In order to assess the importance of the *cis* states in the creation of the surface relief, the amorphous polyester film was irradiated at 351 nm from a krypton laser at an intensity of approximately 3 W/cm^2 for 120-300 s. At this wavelength, only *trans-cis* isomerization take place. A lifetime on the order of 2 hours has been found for the *cis* state in the polyester. For both horizontal and vertical polarizations, only weak peaks ($\sim 15 \text{ nm}$) in the irradiated area were observed.

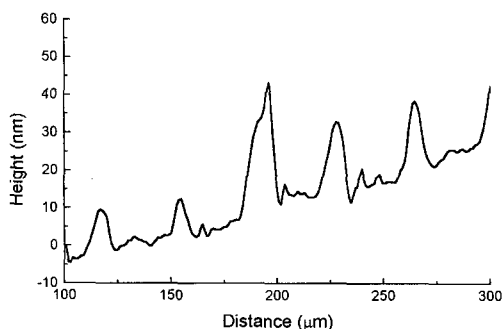


Fig.12: A profiler scan of the amorphous polymer **P6aA** irradiated through the transmission mask. The scan is performed at the edge of the irradiating gaussian profile.

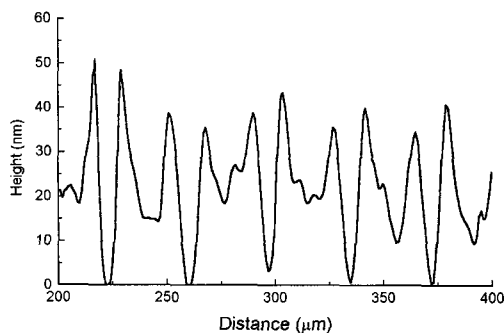


Fig. 13: A profiler scan of the amorphous polymer **P6aA** irradiated through the transmission mask. The scan is performed at halfway to the maximum of the irradiating gaussian profile.

Theory

Initially a theory based on thermal effects was put forward by Barrett et al.¹¹⁾. Later on they modified their proposal to incorporate *trans-cis* free-volume changes which appear as pressure effects^{37,38)}. Lefin et al. proposed an optically controlled anisotropic diffusion model³⁹⁾, in which it is surmised that when an azobenzene molecule goes through a *trans-cis* cycle, it moves in a direction parallel to itself. It is noteworthy that this mechanism can only explain the dispersion of the material (i.e., trenches) and not accumulation (peaks). Pedersen et al.⁴⁰⁾ proposed an empirical model based on mean-field theory. In this case, it was assumed that the interaction between the side chains is mesogenic and thus subject to a form of Maier-Saupe potential. As the chromophores in a side-to-side arrangement attract each other more than in a end-to-end configuration, the accumulation of mass in an area irradiated with light

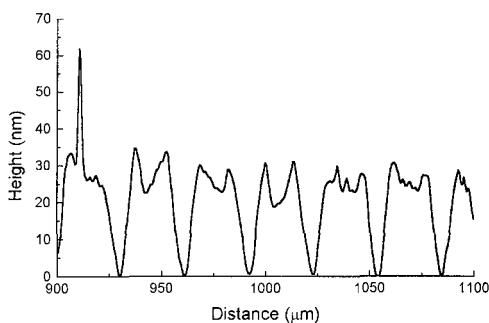


Fig. 14: A profiler scan of the amorphous polymer **P6aA** irradiated through the transmission mask. The scan is performed at the maximum of the irradiating gaussian profile.

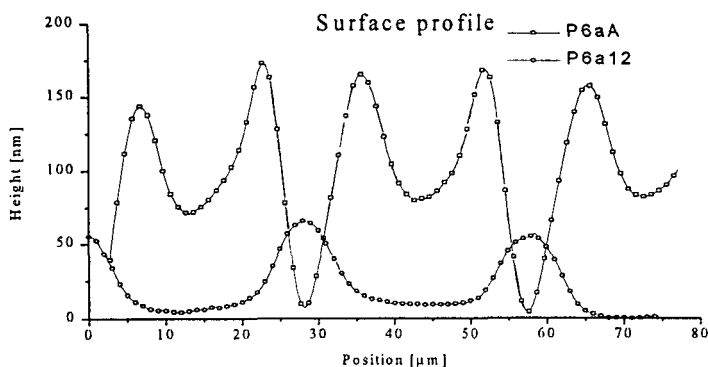


Fig. 15: Surface relief in an aliphatic liquid crystalline (**P6a12**) and an amorphous aromatic (**P6aA**) azobenzene polyester. 5 μm transparent regions are centered at 30 and 60 μm positions.

polarized parallel to the grating vector can be explained. Forces of surface tension counteract this process. This theory explains only the presence of peaks and not valleys. A theory based on gradient forces attributed to dipoles interacting with the gradient of the electric field present in the polymer material has been proposed by Kumar et al.⁴¹⁾. This is based on the claim that orthogonal polarizations do not record appreciable surface relief grating. Our observations show that it is indeed possible to produce large surface relief with orthogonal polarization.

No doubt the surface relief is initiated through the *trans-cis* isomerization cycles, as the only photosensitive component in the polymer is the azobenzene. However, an examination of Figures 10-15 also shows that more than one mechanism must be involved in the mass transport, which depends strongly on the polarization and intensity (fluence) of the laser beam. We believe that in addition to the short range Lennard-Jones interactions, long range electrostatic interactions must be taken into account. Perhaps the ordering of the dipoles in the different systems due to light and the interaction between them may be able to explain the observed phenomena.

Conclusions

We have performed a series of time resolved spectroscopic measurements on substituted azobenzene chromophores, and found strong indications that multiple states are involved in the decay process. A scheme describing the observed decay from $S_2(\pi-\pi^*)$ excited azobenzene consistent with previous observations is proposed. We have found that the decay of the induced anisotropy does depend on the substituent, and also that the attachment of the chromophore to the side chain causes the decay of the anisotropy to slow down. It would be interesting to redo these measurements with a somewhat larger pulse energy, in order to enable to measure the absolute values of $\Delta A/I_{\text{pump}}$ as this would enable us to extract much more information. In order to verify the proposed decay scheme, the experiments should also be performed by just pumping the S_1 state.

The appearance of a surface relief when a thin film of an azobenzene polymer is irradiated with polarized light is a remarkable process. This process is definitely amplified by the attachment of the azobenzene to main or side chains of a polymer. On the one hand, free-volume requirements when the molecule undergoes a *trans-cis* isomerization may not be

unimportant in the formation of topographic features, we believe that more subtle interactions between the dipolar azobenzenes have to be taken into account. An understanding of this process will lead to easy methods of replication, which are very important in the fields of microelectronics and microoptics. Technically, we have been successful in replicating the surface relief gratings many times using a silicone elastomer mould.

Acknowledgments

N. C. R. Holme thanks the Carlsberg Foundation and the Danish Natural Science Research Council for financial aid. This project has been supported by the Danish Materials Technology Development Programme (MUP2), the Danish Natural Science Research Council, and Danish Research Academy. The authors are also extremely grateful to Prof. A. Natansohn and Prof. P. Rochon for supplying the polymer pDR1A.

References

T. B. Norris is with the University of Ann Arbor, Michigan, U. S. A

L. Nikolova is with the Bulgarian Academy of Sciences, Sofia, Bulgaria

- ¹⁾ C. V. Shank, *Femtochem. Femtobiol.: Ultrafast React. Dyn. At.-Scale Resolut.*, Nobel Symp. Ed: V. Sundström, Imperial College Press, London, U.K., **101**, 660 (1997)
- ²⁾ H. Rau, *Angew. Chem.* **85**, 248 (1973)
- ³⁾ M. Eich, J. H. Wendorff, B. Reck, H. Ringsdorf, *Makromol. Chem. Rapid Commun.* **8**, 59 (1987)
- ⁴⁾ U. Wiesner, M. Antonietti, C. Boeffel, H. W. Spiess, *Makromol. Chem.* **191**, 2133 (1990)
- ⁵⁾ V. P. Shibaev, I. V. Yakolev, S. G. Kostromin, S. A. Ivanov, T. I. Sverkova, *Vysokomol. soyed.* **A32**, 1552 (1990)
- ⁶⁾ A. Natansohn, P. Rochon, J. Gosselin, S. Xie, *Macromolecules* **25**, 2268 (1992)
- ⁷⁾ Th. Fischer, L. Läscher, J. Stumpe, S. G. Kostromin, *J. Photochem. Photobiol. A: Chem.* **80**, 453 (1994)
- ⁸⁾ H. H. Haitjema, G. L. von Morgen, Y. Y. Tan, G. Challa, *Macromolecules* **27**, 6201 (1994)
- ⁹⁾ Z. Sekkat, M. Büchel, H. Orendi, H. Menzel, W. Knoll, *Chem. Phys. Lett.* **220**, 497 (1994)
- ¹⁰⁾ M. Schönhoff, L. F. Chi, H. Fuchs, M. Lösche, *Langmuir*, **11**, 163 (1995)
- ¹¹⁾ P. Rochon, E. Batalla, A. Natansohn, *Appl. Phys. Lett.* **66**, 136 (1995)
- ¹²⁾ D. Y. Kim, S. K. Tripathy, L. Li, J. Kumar, *Appl. Phys. Lett.* **66**, 1166 (1995)
- ¹³⁾ P. S. Ramanujam, N. C. R. Holme, S. Hvilsted, *Appl. Phys. Lett.* **68**, 1329 (1996)
- ¹⁴⁾ P. S. Ramanujam, N. C. R. Holme, L. Nikolova, R. H. Berg, S. Hvilsted, E. T. Kristensen, C. Kulinna, A. B. Nielsen, M. Pedersen, *Proc. SPIE*, **3011**, 319 (1997)
- ¹⁵⁾ M. Pedersen, Ph. D. Thesis, The Technical University of Denmark (1997)
- ¹⁶⁾ S. Hvilsted, F. Andruzzi, C. Kulinna, H. W. Siesler, P. S. Ramanujam, *Macromolecules* **28**, 2172 (1995)
- ¹⁷⁾ L. Andruzzi, A. Altomare, F. Ciardelli, R. Solaro, S. Hvilsted, P. S. Ramanujam, submitted to *Macromolecules* (1998)
- ¹⁸⁾ R. H. Berg, S. Hvilsted, P. S. Ramanujam, *Nature*, **383**, 505 (1996)

- 19) A. Natansohn, P. Rochon, J. Gosselin, S. Xie, *Macromolecules* **25**, 2268 (1992).
- 20) R.N. Camp, I. R. Epstein, C. Steel, *J. Am. Chem. Soc.* **99**, 2453 (1997)
- 21) G. Olbrich, *Chem. Phys.* **27**, 117 (1978)
- 22) H. J. Rau, *J. Photochem.*, **26**, 221 (1984)
- 23) S. Monti, G. Orlandi, P. Palmieri, *Chem. Phys.* **71**, 87 (1982)
- 24) T. G. Pedersen, P. S. Ramanujam, P. M. Johansen, S. Hvilsted, *J. Opt. Soc. Am. B* in press (1998).
- 25) I. K. Lednev, T-Q. Ye, R.E. Hester, J. N. Moore, *J. Phys. Chem.* **100**, 13338 (1997)
- 26) W. S. Struve, *Chem. Phys. Lett.* **46**, 15 (1977)
- 27) C. G. Morgante, W. S. Struve, *Chem. Phys. Lett.* **68**, 267 (1979)
- 28) P. Hamm, S. M. Ohline, W. Zinth, *J. Chem. Phys.* **106**, 519 (1997)
- 29) J. K. Rhee, T.S. Sosnowski, T. B. Norris, J. A. Arns, W. S. Colburn, *Opt. Lett.* **19**, 1550 (1994)
- 30) T. B. Norris, *Opt. Lett.* **17**, 1009 (1992)
- 31) N. Biswas, S. Umapathy, *J. Chem. Phys.* **107**, 7849 (1997)
- 32) P. Bortolus, S. Monti, *J. Phys. Chem.* **83**, 648 (1979)
- 33) N. C. R. Holme, R. H. Berg, S. Hvilsted and P. S. Ramanujam (to be published)
- 34) N. C. R. Holme, Ph. D. Thesis, Risø National Laboratory, Roskilde Denmark, Risø-R-983 (EN), (1997); N. C. R. Holme, L. Nikolova, P. S. Ramanujam, S. Hvilsted, *Appl. Phys. Lett.* **70**, 1518 (1997)
- 35) I. Naydenova, L. Nikolova, T. Todorov, N. C. R. Holme, P. S. Ramanujam, S. Hvilsted, *J. Opt. Soc. Am. B*, **15**, 10257 (1998)
- 36) X. L. Jiang, L. Li, J. Kumar, D. Y. Kim, V. Shivshankar, S. K. Tripathy, *Appl. Phys. Lett.* **68**, 2618 (1996)
- 37) C. Barrett, A. Natansohn, P. Rochon, *J. Phys. Chem.* **100**, 8836 (1996)
- 38) C. Barrett, P. L. Rochon, A. L. Natansohn, *J. Chem. Phys.* **109**, 1505 (1998)
- 39) P. Lefin, C. Fiorini, J. M. Nunzi, *Pure Appl. Opt.* **7**, 71 (1998)
- 40) T. G. Pedersen, P. M. Johansen, N. C. R. Holme, P. S. Ramanujam, S. Hvilsted, *Phys. Rev. Lett.* **80**, 89 (1998)
- 41) J. Kumar, L. Li, X. L. Jiang, D. Y. Kim, T. S. Lee, S. Tripathy, *Appl. Phys. Lett.* **72**, 2096 (1998)